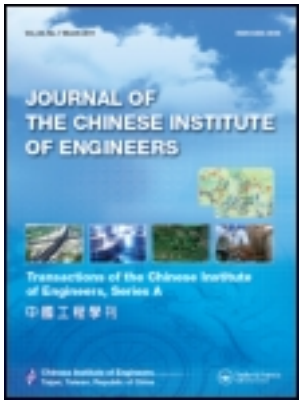

Journal of the Chinese Institute of Engineers
Publication details, including instructions for authors and subscription information:
http://www.tandfonline.com/loi/tcie20

Modeling nonlinear rate dependent behaviors of composite laminates

Jia-Lin Tsai [a] & Hamvey Wang [b]

[a] Department of Mechanical Engineering , National Chiao Tung University , Hsinchu 300, Taiwan Phone: 886-3-5731608 Fax: 886-3-5731608 E-mail:

[b] Department of Mechanical Engineering , National Chiao Tung University , Hsinchu 300, Taiwan

Published online: 04 Mar 2011.

To cite this article: Jia-Lin Tsai & Hamvey Wang (2007) Modeling nonlinear rate dependent behaviors of composite laminates, Journal of the Chinese Institute of Engineers, 30:1, 141-148, DOI: 10.1080/02533839.2007.9671237

To link to this article: http://dx.doi.org/10.1080/02533839.2007.9671237

MODELING NONLINEAR RATE DEPENDENT BEHAVIORS OF COMPOSITE LAMINATES

Jia-Lin Tsai* and Hamvey Wang

ABSTRACT

This study aims to propose a simple explicit model for predicting the nonlinear rate dependent behaviors of composite laminates. Using one parameter plastic potential to describe the flow rule, the viscoplasticity model is expressed as a single master effective stress-effective plastic strain curve in the form of a power law with a rate dependent amplitude. Based on the viscoplasticity model together with the laminated plate theory, the incremental form of the constitutive formulation is derived to model the nonlinear rate dependent behaviors of composite laminates. Symmetric glass/epoxy and graphite/epoxy composite laminates were tested at three different strain rates and the experimental results were then compared with the model predictions. It was indicated that the proposed constitutive model is effective in characterizing the nonlinear rate dependent behaviors of composite laminates at strain levels up to 1%.

Key Words: composite laminates, mechanical properties, strain rate.

I. INTRODUCTION

Unidirectional polymeric composites exhibit nonlinear rate dependent behaviors when subjected to dynamic off-axis loading. Similarly, for composite laminates consisting of plies with different fiber orientations, the constitutive behaviors may also demonstrate rate sensitivity. Due to the anisotropic characteristics of composites, it is a challenging task to develop a constitutive model accounting for the nonlinear rate dependent behaviors. In past decades, the rate effect on composite materials has been investigated and characterized by many researchers. Hosur *et al.*, (2001) studied strain rate effect on carbon/epoxy composite laminates and found that the stress-strain curves become stiffening when the strain rate increases. Gates and Sun (1991) and Yoon and Sun (1991) adopted one parameter plastic potential in conjunction with the overstress concept to model the elastic/viscoplastic behavior of unidirectional fiber composites. The strain rate ranges in their analysis were from 10^{-6}/s to 10^{-3}/s. Sun and Zhu (2000) employed the overstress viscoplasticity model incorporated with the laminated plate theory to predict the constitutive relations of symmetric balanced laminates at various strain rates. However, their analysis is pretty cumbersome, since it is necessary to determine five parameters in the overstress viscoplasticity model as well as to solve a nonlinear ordinary differential equation. The effects of the residual stress and deformation-induced fiber orientation change on the nonlinear behavior were also taken into account in their studies. Thiruppukuzhi and Sun (2001) characterized the rate dependent behavior of unidirectional glass/epoxy composites and woven E-glass fabric using a three parameter viscoplasticity model. With the assistance of the finite element method, the three parameter viscoplasticity model was employed to predict the stress and strain relation of composite laminates at various strain rates. By performing high strain rate testing on off-axis composite specimens using a Split Hopkinson Pressure Bar, Tsai and Sun (2002) indicated that the three parameter viscoplasticity model, although established based on low strain rate tests, was suitable for modeling high strain rate responses of unidirectional composites. In view of the forgoing, most efforts were made on the modeling of unidirectional composites, while few studies concerning the nonlinearity rate sensitivity of laminates have been reported.

*Corresponding author. (Tel: 886-3-5731608; Fax: 886-3-5720634; Email: jialin@mail.nctu.edu.tw)

The authors are with the Department of Mechanical Engineering, National Chiao Tung University, Hsinchu 300, Taiwan.

In this research, a simple explicit constitutive model was proposed for characterizing the rate sensitivity of laminates. The three parameter viscoplasticity model was employed in conjunction with the laminated plate theory to establish the stress and strain relations of composite laminates. Through a numerical iteration of the incremental form of constitutive formulations, the stress and strain relations of composite laminates at various strain rates were generated. In order to verify the model predictions, symmetric glass/epoxy and graphite/epoxy laminates were tested at three different strain rates. The experimental data were then compared with the model predictions.

II. VISCOPLASTICITY MODEL

In order to model the nonlinear rate dependent behavior of unidirectional composites, the one parameter plastic potential

$$f = \frac{1}{2}(\sigma_{22}^2 + 2a_{66}\sigma_{12}^2), \tag{1}$$

proposed by Sun and Chen (1989) for modeling 2-D static nonlinear behavior of composites was employed to develop the viscoplasticity model. In Eq. (1), a_{66} is an orthotropy coefficient, and σ_{ij} are stress components referred to the material principal directions. For small deformations, the total strain rates can be decomposed into elastic and plastic parts as

$$\dot{\varepsilon}_{ij} = \dot{\varepsilon}_{ij}^e + \dot{\varepsilon}_{ij}^p. \tag{2}$$

Using the one parameter plastic potential to model the associated flow rule, the explicit form of plastic strain rate is expressed as

$$\begin{Bmatrix} \dot{\varepsilon}_{11}^p \\ \dot{\varepsilon}_{22}^p \\ \dot{\gamma}_{12}^p \end{Bmatrix} = \begin{Bmatrix} 0 \\ \sigma_{22} \\ 2a_{66}\sigma_{12} \end{Bmatrix} \dot{\lambda}, \tag{3}$$

where $\dot{\lambda}$ is a proportional factor.

Define the effective stress as

$$\bar{\sigma} = \sqrt{3f} = \sqrt{\frac{3}{2}}(\sigma_{22}^2 + 2a_{66}\sigma_{12}^2)^{1/2}. \tag{4}$$

Through the equivalence of plastic work rate

$$\dot{w}^p = \sigma_{ij}\dot{\varepsilon}_{ij}^p = \bar{\sigma}\,\dot{\bar{\varepsilon}}^p = 2f\dot{\lambda}, \tag{5}$$

the effective plastic strain rate is written as

$$\dot{\bar{\varepsilon}}^p = \sqrt{\frac{2}{3}}[(\dot{\varepsilon}_{22}^p)^2 + \frac{1}{2a_{66}}(\dot{\gamma}_{12}^p)^2]^{1/2}, \tag{6}$$

and the proportional factor $\dot{\lambda}$ is given as

$$\dot{\lambda} = \frac{3}{2}\frac{\dot{\bar{\varepsilon}}^p}{\bar{\sigma}} = \frac{3}{2}\frac{\dot{\bar{\sigma}}}{H_p\bar{\sigma}}, \tag{7}$$

where

$$H_p = \frac{\dot{\bar{\sigma}}}{\dot{\bar{\varepsilon}}^p}, \tag{8}$$

is the rate dependent plastic modulus.

The viscoplasticity model developed by Tsai and Sun (2002) is expressed in the form

$$\bar{\varepsilon}^p = \chi(\dot{\bar{\varepsilon}}^p)^m(\bar{\sigma})^n, \tag{9}$$

where χ, m, and n are the material constants in the viscoplasticity model. The determination of the material constants for S2/8552 glass/epoxy and graphite/epoxy composites will be presented in the next section. With this viscoplasticity model, the rate dependant plastic modulus H_p is deduced as

$$H_p = \frac{\dot{\bar{\sigma}}}{\dot{\bar{\varepsilon}}^p} = \frac{\dot{\bar{\sigma}}dt}{\dot{\bar{\varepsilon}}^p dt} = \frac{d(\bar{\sigma})}{d\bar{\varepsilon}^p} = \frac{1}{n\chi(\dot{\bar{\varepsilon}}^p)^m(\bar{\sigma})^{n-1}}. \tag{10}$$

It is noted that the rate dependent plastic modulus H_p is a function of effective stress and effective plastic strain rate. According to the definition of the effective stress given in Eq. (4), $\dot{\bar{\sigma}}$ is derived as

$$\dot{\bar{\sigma}} = \frac{1}{\bar{\sigma}}\{\frac{3}{2}\sigma_{22}\dot{\sigma}_{22} + 3a_{66}\sigma_{12}\dot{\sigma}_{12}\}. \tag{11}$$

By substituting Eq. (11) together with Eq. (7) into Eq. (3), the plastic strain rates are expressed explicitly as

$$\begin{Bmatrix} \dot{\varepsilon}_{11}^p \\ \dot{\varepsilon}_{22}^p \\ \dot{\gamma}_{12}^p \end{Bmatrix} = \begin{bmatrix} 0 & 0 & 0 \\ 0 & \frac{9\sigma_{22}^2}{4H_p\bar{\sigma}^2} & \frac{9a_{66}\sigma_{22}\sigma_{12}}{2H_p\bar{\sigma}^2} \\ 0 & \frac{9a_{66}\sigma_{22}\sigma_{12}}{2H_p\bar{\sigma}^2} & \frac{9a_{66}^2\sigma_{12}^2}{H_p\bar{\sigma}^2} \end{bmatrix} \begin{Bmatrix} \dot{\sigma}_{11} \\ \dot{\sigma}_{22} \\ \dot{\sigma}_{12} \end{Bmatrix}. \tag{12}$$

With the inclusion of the elastic parts, the incremental form of stress and strain relation for unidirectional composites is given as

$$\begin{Bmatrix} \dot{\varepsilon}_{11} \\ \dot{\varepsilon}_{22} \\ \dot{\gamma}_{12} \end{Bmatrix} = \begin{bmatrix} S_{11} & S_{12} & 0 \\ S_{12} & S_{22} + \frac{9\sigma_{22}^2}{4H_p\bar{\sigma}^2} & \frac{9a_{66}\sigma_{22}\sigma_{12}}{2H_p\bar{\sigma}^2} \\ 0 & \frac{9a_{66}\sigma_{22}\sigma_{12}}{2H_p\bar{\sigma}^2} & S_{66} + \frac{9\sigma_{66}^2\sigma_{12}^2}{H_p\bar{\sigma}^2} \end{bmatrix} \begin{Bmatrix} \dot{\sigma}_{11} \\ \dot{\sigma}_{22} \\ \dot{\sigma}_{12} \end{Bmatrix}$$

$$= [S^{ep}] \begin{Bmatrix} \dot{\sigma}_{11} \\ \dot{\sigma}_{22} \\ \dot{\sigma}_{12} \end{Bmatrix}, \tag{13}$$

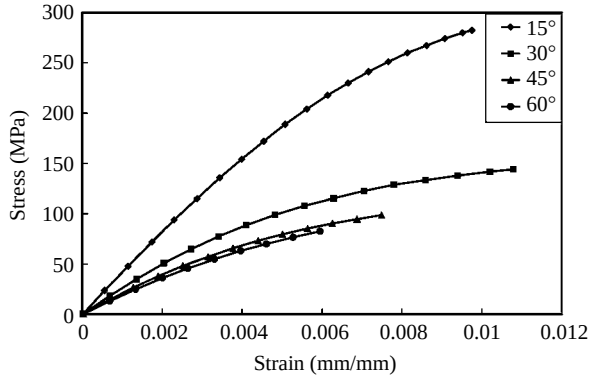

Fig. 1 Stress-strain curves for glass/epoxy composites at strain rate 0.0001/s

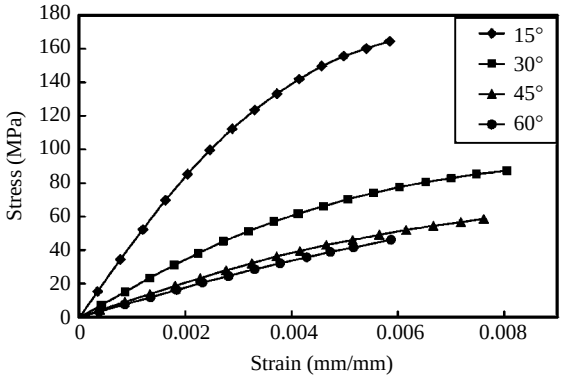

Fig. 2 Stress-strain curves for graphite/epoxy composites at strain rate 0.0001/s

where S_{ij} are elastic compliances of the composite (Gibson, 1994). It is noted that the constitutive relation relies on the current stress states as well as the effective plastic strain rate and a numerical iteration is required to compute these stress and plastic strain variables.

III. PARAMETER DETERMINATION

To completely model the rate dependent response of composites, the orthotropy coefficient a_{66} in the plastic potential function and the associated parameters in the viscoplasticity model need to be determined. This can be accomplished by performing tensile tests on the off-axis coupon specimens at different strain rates. Both glass/epoxy composites (S2/8552 prepreg from Hexcel, USA) and graphite/epoxy composites (CFA prepreg with Toho HTA graphite fiber from AD Group, Taiwan) were examined in this study. Twenty-four plies unidirectional glass/epoxy composites and ten plies unidirectional graphite/epoxy composites were laid up manually and then cured, using the recommended curing process. Off-axis composite coupon specimens with fiber orientations of 15° 30°, 45° and 60° were cut from the composite panels using a diamond saw. Since the 0° specimen generally is not sensitive to strain rate and the 90° specimen has very short nonlinear deformation, neither was included in the parameter determination. Glass/epoxy end tabs, 25 mm in length, were bounded, resulting in specimens with 100 mm gage length and 17.8 mm width. The thicknesses measured at the center of the specimens for the glass/epoxy and graphite/epoxy composites were 1.8 mm and 1.5 mm respectively. Back to back axial strain gages were mounted at the centers of the specimens to measure the strain histories. Tensile tests were conducted on a hydraulic MTS 810 testing machine with stroke control at three different strain rates of 0.0001, 0.01 and 1/s. During the tests, the load and strain histories were recorded using a LabView data acquisition system with a computer. Figs. 1 and 2 depict the stress and strain curves of S2/8552 glass/epoxy composites and graphite/epoxy composites at a strain rate of 0.0001/s, respectively. It is noted that the ending point of each curve represents the failure of the associated specimen.

For off-axis specimens subjected to uniaxial monotonic loading, the effective stress and effective plastic strain can be related to the uniaxial applied stress σ_x and plastic strain ε_x^p as (Thiruppukuzhi and Sun, 2001)

$$\bar{\sigma} = h(\theta)\sigma_x, \tag{14}$$

$$\bar{\varepsilon}^p = \frac{\varepsilon_x^p}{h(\theta)}, \tag{15}$$

where $h(\theta)$ is an off-axis parameter defined as

$$h(\theta) = \sqrt{\frac{3}{2}}[\sin^4\theta + 2a_{66}\sin^2\theta\cos^2\theta]^{1/2}, \tag{16}$$

where θ is the off-axis angle with respect to loading direction..

It is noted that the axial plastic strain ε_x^p was obtained by subtracting the elastic part from the total measured axial strain ε_x With Eq. (14) and Eq. (15), the effective stress and effective plastic strain can be obtained from the experimentally determined axial stress and axial plastic strain. For a given strain rate, the effective stress-effective plastic strain relation, based on the equivalence of plastic work, should be unique in monotonic loading. Thus, the proper value of a_{66} was chosen by trial and error such that the stress-plastic strain curves measured from different fiber orientations collapse into a single effective stress-effective plastic strain curve. The master effective stress-effective plastic strain curves were then fitted by a power law as

$$\bar{\varepsilon}^p = A(\bar{\sigma})^n. \tag{17}$$

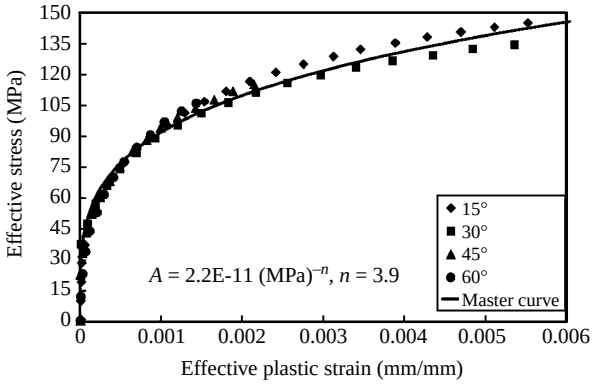

Fig. 3 Effective stress-effective plastic strain curves for glass/epoxy composites at strain rate 0.0001/s

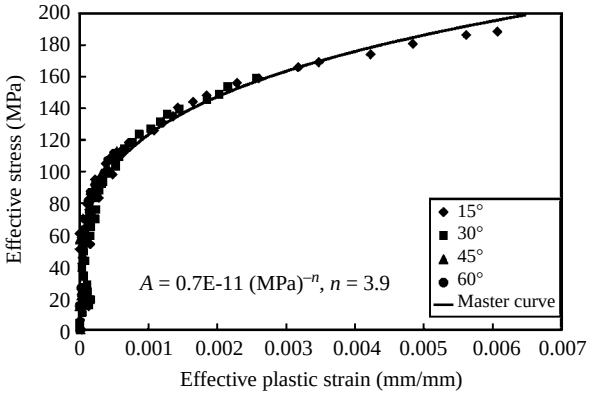

Fig. 5 Effective stress-effective plastic strain curves for glass/epoxy composites at strain rate 1/s

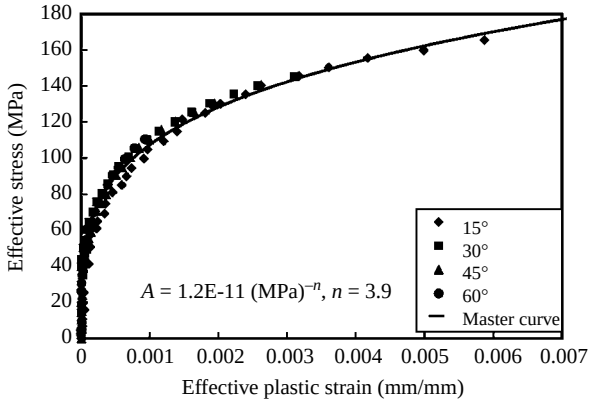

Fig. 4 Effective stress-effective plastic strain curves for glass/epoxy composites at strain rate 0.01/s

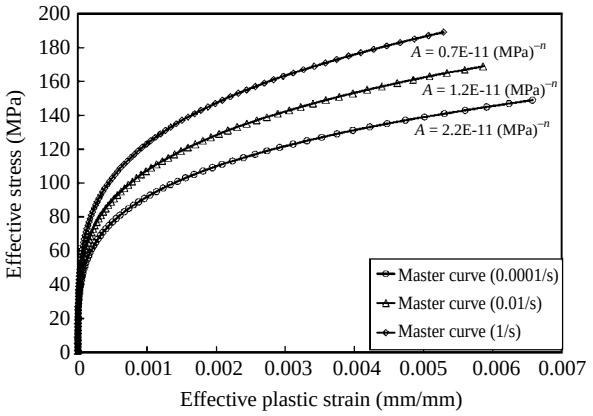

Fig. 6 Master effective stress and effective plastic strain curves for glass/epoxy composites at strain rates of 0.0001/s, 0.01/s and 1/s

Figure 3 illustrates the collapsed effective stress-effective plastic strain curves and the power law-fitted master curve for glass/epoxy composites at strain rate 0.0001/s with $a_{66} = 1.4$. Similar procedures were performed on the experimental data with strain rates 0.01/s and 1/s, and the results are shown in Figs. 4 and 5, respectively. The master curves corresponding to the three different strain rates are summarized in Fig. 6. Experimental observations indicated that the power n in the power law of Eq. (17) is constant for all the strain rates considered. However, the amplitude A is a function of the effective plastic strain rate $\bar{\varepsilon}^p$. Again, a power law is chosen to describe the rate dependent coefficient A as

$$A = \chi(\bar{\varepsilon}^p)^m \tag{18}$$

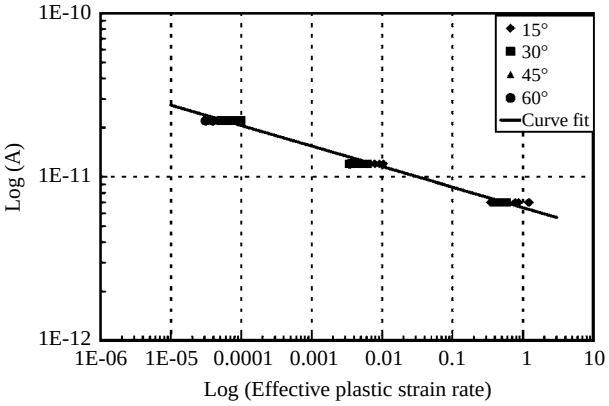

Fig. 7 Logarithmic plot of the amplitude A versus effective plastic strain rate for glass/epoxy composites

Fig. 7 shows amplitude A as a function of the effective plastic strain rate on a log-log scale for the composite. The parameters χ and m were determined from these plots as the intercept and the slope, respectively. The values of the parameters in the viscoplasticity model together with elastic material constants for S2/8552 glass/epoxy composite are listed in Table 1. It is noted that although the coefficient A is determined based on low strain rate ranges, it can be extended into high strain rate (Tsai and Sun, 2002). In the same manner, the master curves for graphite/epoxy composites at different strain rates

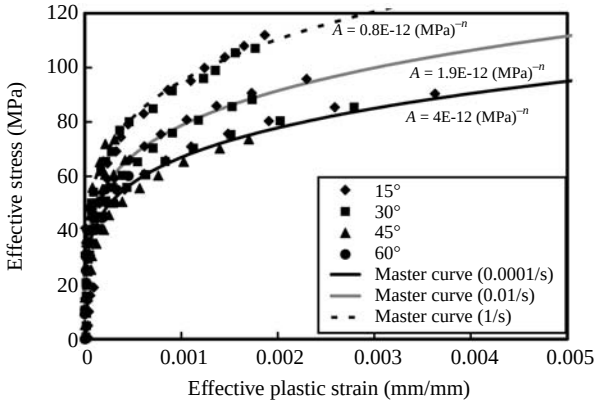

Fig. 8 Master effective stress and effective plastic strain curves for graphite/epoxy composites at strain rates of 0.0001/s, 0.01/s and 1/s

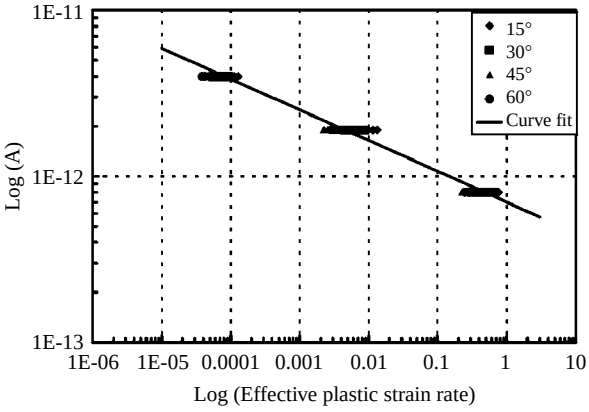

Fig. 9 Logarithmic plot of the amplitude A versus effective plastic strain rate for graphite/epoxy composites

were produced and the results were summarized in Fig. 8 with a_{66} =1.6. Again, a log-log plot was generated in Fig. 9 for the determination of the parameters in the viscoplasticity model. All material constants for graphite/epoxy composites are presented in Table 2.

IV. MODELING COMPOSITES LAMINATES

In order to model the nonlinear rate dependent behaviors of composite laminates, the incremental form of the stress and strain relations provided in Eq. (13) was employed in the analysis. By inverting Eq. (13), the incremental form of the constitutive relations is expressed as

$$\begin{Bmatrix} \dot{\sigma}_{11} \\ \dot{\sigma}_{22} \\ \dot{\sigma}_{12} \end{Bmatrix} = [Q^{ep}] \begin{Bmatrix} \dot{\varepsilon}_{11} \\ \dot{\varepsilon}_{22} \\ \dot{\gamma}_{12} \end{Bmatrix}, \tag{19}$$

where $[Q^{ep}]$ is the elastic-plastic stiffness matrix. In

Table 1 Material properties and parameters for the viscoplasticity model for S2/8552 glass/epoxy composites

E_1(GPa)	55.7
E_2(GPa)	21.5
G_{12}(GPa)	6.9
v_{12}	0.29
a_{66}	1.4
n	3.9
χ(MPa)$^{-n}$	6.50E–12
m	–0.125
$\alpha_1(10^{-6}/°C)$	7.0
$\alpha_2(10^{-6}/°C)$	18.3

Table 2 Material properties and parameters for the viscoplasticity model for CFA graphite/epoxy composites

E_1(GPa)	138.5
E_2(GPa)	8.1
G_{12}(GPa)	4.2
v_{12}	0.27
a_{66}	1.6
n	4.6
χ(MPa)$^{-n}$	0.70E–12
m	–0.185
$\alpha_1(10^{-6}/°C)$	0.57
$\alpha_2(10^{-6}/°C)$	41.4

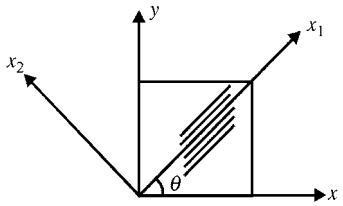

Fig. 10 Coordinate Transformation

general, the coordinate system ($x - y$ system) is set up, which does not always coincide with the material principal direction ($x_1 - x_2$ system) as illustrated in Fig. 10. Through the coordinate transformation law, the constitutive formulations in $x - y$ coordinate system become

$$\begin{Bmatrix} \dot{\sigma}_{xx} \\ \dot{\sigma}_{yy} \\ \dot{\sigma}_{xy} \end{Bmatrix} = [T_\sigma]^{-1}[Q^{ep}][T_\varepsilon] \begin{Bmatrix} \dot{\varepsilon}_{xx} \\ \dot{\varepsilon}_{yy} \\ \dot{\gamma}_{xy} \end{Bmatrix} = [Q^{ep}] \begin{Bmatrix} \dot{\varepsilon}_{xx} \\ \dot{\varepsilon}_{yy} \\ \dot{\gamma}_{xy} \end{Bmatrix}, \tag{20}$$

where

$$[T_\varepsilon] = \begin{bmatrix} \cos^2\theta & \sin^2\theta & \sin\theta\cos\theta \\ \sin^2\theta & \cos^2\theta & -\sin\theta\cos\theta \\ -2\sin\theta\cos\theta & 2\sin\theta\cos\theta & \cos^2\theta - \sin^2\theta \end{bmatrix}, \tag{21}$$

$$[T_\sigma] = \begin{bmatrix} \cos^2\theta & \sin^2\theta & 2\sin\theta\cos\theta \\ \sin^2\theta & \cos^2\theta & -2\sin\theta\cos\theta \\ -\sin\theta\cos\theta & \sin\theta\cos\theta & \cos^2\theta - \sin^2\theta \end{bmatrix}, \tag{22}$$

For composite laminates containing many plies with various fiber orientations, Eq. (20) can be recognized as the constitutive formulation of the k_{th} ply and re-written as

$$\begin{Bmatrix} \dot{\sigma}_{xx} \\ \dot{\sigma}_{yy} \\ \dot{\sigma}_{xy} \end{Bmatrix}_k = [\overline{Q}^{ep}]_k \begin{Bmatrix} \dot{\varepsilon}_{xx} \\ \dot{\varepsilon}_{yy} \\ \dot{\gamma}_{xy} \end{Bmatrix}_k . \tag{23}$$

It is noted that when the symmetric laminates are subjected to in-plane loading, the strain components on each ply are the same and equal to those in the mid-plane. However, the stress states in the laminate are, in general, discontinuous across the ply interfaces due to different material properties resulting from different fiber orientations. Summation of Eq. (23) through the thickness yields the relation between the resultant force of the whole laminate and the mid-plane strain as

$$\begin{Bmatrix} \dot{N}_x \\ \dot{N}_y \\ \dot{N}_{xy} \end{Bmatrix} = \sum_k [\overline{Q}^{ep}]_k h_k \begin{Bmatrix} \dot{\varepsilon}_{xx} \\ \dot{\varepsilon}_{yy} \\ \dot{\gamma}_{xy} \end{Bmatrix} = [A] \begin{Bmatrix} \dot{\varepsilon}_{xx} \\ \dot{\varepsilon}_{yy} \\ \dot{\gamma}_{xy} \end{Bmatrix}, \tag{24}$$

where h_k is the thickness of the k_{th} ply and $\{\dot{N}\}$ is the incremental form of the resultant force defined as

$$\begin{Bmatrix} \dot{N}_x \\ \dot{N}_y \\ \dot{N}_{xy} \end{Bmatrix} = \sum_k h_k \begin{Bmatrix} \dot{\sigma}_{xx} \\ \dot{\sigma}_{yy} \\ \dot{\sigma}_{xy} \end{Bmatrix}_k . \tag{25}$$

Inverting Eq. (24), we obtained the constitutive equation for the laminates as

$$\begin{Bmatrix} \dot{\varepsilon}_{xx} \\ \dot{\varepsilon}_{yy} \\ \dot{\gamma}_{xy} \end{Bmatrix} = [A]^{-1} \begin{Bmatrix} \dot{N}_x \\ \dot{N}_y \\ \dot{N}_{xy} \end{Bmatrix}. \tag{26}$$

Thus, for a given loading history, the associated stress and strain relation of the laminate can be established from Eq. (26) using a numerical iteration.

V. NUMERICAL PROCEDURE

When composite laminates are subjected to in-plane loading, the in-plane deformation of each ply in the global coordinate is the same. However, in the material principal coordinate, because of different fiber orientation, the corresponding strain components and the strain rates at each ply are different. Moreover, the effective plastic strain rates calculated, based on the strain rates in the material principal directions, are also different. It is noted that the ply constitutive formulations given by Eq. (13) are dependent on the effective plastic strain rate and the stress state. Therefore, to construct the constitutive relation of the laminates from the ply constitutive formulations, it is required to calculate the effective plastic strain rate and the corresponding stress states in each ply.

For a given tiny loading increment, the strain increments of the laminates in the $x - y$ coordinate were calculated from Eq. (26) and the results were then recognized as the strain increments in each ply. Using the ply constitutive equation given in Eq. (23), the associated stress increments were evaluated. It is noted that these components are expressed in the $x - y$ coordinate system. Through the coordinate transformation law, the stress and strain increments in the material principal directions were calculated. By subtracting the elastic part from the total strain increment, the plastic strain increments in the individual ply were obtained and the effective plastic strain rates were then computed using Eq. (6). On the other hand, the stress states were updated by adding all of the previous calculated stress increments. The effective stress was then calculated from Eq. (4). Once the stress states and the effective plastic strain rates were determined, the incremental form of the constitutive relation in Eq. (13) was generated. By summing the individual ply properties over the thickness, the constitutive matrix [A] in Eq. (24) for the laminates was updated and utilized for the estimation of the strain increments in the next stage. The strain increment with regard to a load increment was evaluated with Eq. (26) and the total strain was obtained from the addition of all previous strain increments. By performing the forgoing numerical iteration together with the loading histories as input, the stress and strain curves of the composite laminates at various strain rates were established.

For unidirectional composites, the Coefficients of Thermal Expansion (CTE) just like other material constants are orthotropic. When composite laminates containing numbers of plies with different fiber orientations are fabricated, due to the mismatch of CTE, the thermal residual stresses may be produced in the laminates. The process-induced stresses having an effect on the nonlinear behavior of laminates were included in the analysis. By following the experimental procedures proposed in references (Tuttle, 1989; Lanza di Scalea, 1998), the thermal expansion coefficients, α_1 and α_2, for glass/epoxy composites and graphite/epoxy composites were measured and addressed in Tables 1 and 2, respectively. For glass/epoxy and graphite/epoxy composites, the curing temperatures were 180°C

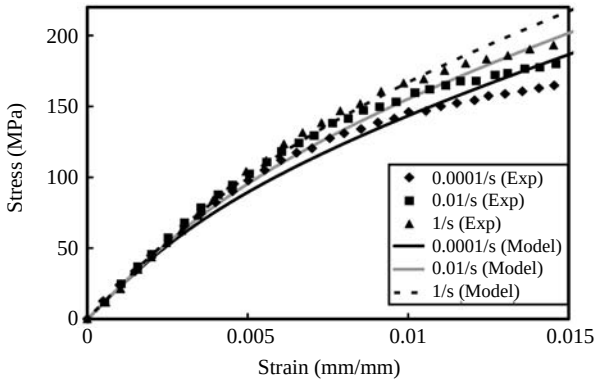

Fig. 11 Comparison of model predictions and experimental stress-strain curves for $[\pm 45/90_2]_{4s}$ glass/epoxy laminates at three different strain rates

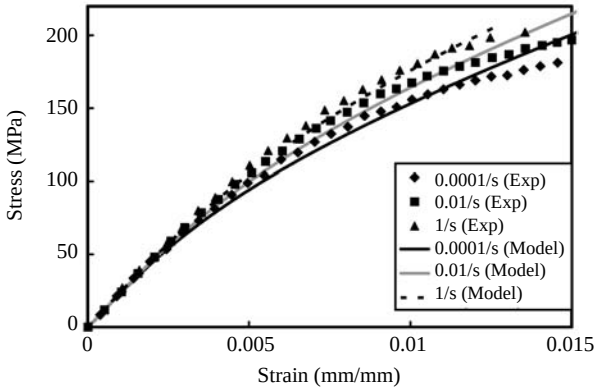

Fig. 12 Comparison of model predictions and experimental stress-strain curves for $[75_2/-60/30]_{4s}$ glass/epoxy laminates at three different strain rates

and 150°C, respectively and the laminates were assumed to be stress free at these temperatures. By using thermal-elastic analysis, the thermal residual stresses of the composites at room temperature (25°C) were computed and then input in the numerical procedure as the initial stress variables for each ply before the mechanical loading was applied.

VI. COMPOSITE LAMINATE TESTING

In order to verify the viscoplasticity model incorporated with the laminated plate theory suitable for characterizing the rate sensitivity of the laminates, tensile tests were carried out on the specimens at different strain rates. Two composite material systems were investigated in this study. One was glass/epoxy composite laminates with stacking sequences of $[\pm 45/90_2]_{4s}$ and $[75_2/-60/30]_{4s}$. The other was graphite/epoxy composites with stacking sequences of $[\pm 45]_{3s}$ and $[60/-30]_{3s}$. It is noted that since 0 degree ply would significantly diminish the nonlinear effect, there are no 0 degree plies contained in the laminates. Moreover, to be consistent, the curing process used for unidirectional composites was employed in the fabrication of the laminates. Coupon specimens with gage length of 100 mm and width of 17.6 mm were cut from the composite panels using a diamond saw. Back to back strain gages were adhered at the centers of the specimens for the strain measurements.

Uniaxial tensile tests were conducted, using a servo-hydraulic MTS machine in stroke control mode with three different constant nominal strain rates of 10^{-4}/s, 10^{-2}/s and 1/s. The nominal strain rate was the stroke rate of the loading frame divided by the original specimen length. During the tests, the true strain was measured by strain gages directly mounted on the specimens. The true strain signals as well as the load signals were recorded using LabView and then employed for the generation of the experimental stress and strain curves.

VII. RESULTS AND DISCUSSION

Figures 11 and 12 depict the experimental stress and strain curves of $[\pm 45/90_2]_{4s}$ and $[75_2/-60/30]_{4s}$ glass/epoxy composite laminates at three different strain rates, respectively. The predictions based on the viscoplasticity model together with laminated plate theory are also included in the figures. It was shown that the nonlinear portions of the stress and strain curves are sensitive to the strain rate. Moreover, when the strain rate increases, the material becomes stiffer. At strain ranges less than 1%, the model predictions demonstrate good agreement with experimental results. However, at higher strain levels, the predictions deviate from the experimental results. This disparity could be attributed to the fact that the parameters used in the viscoplasticity model were determined from the experimental data for the strain level lower than 1%. Thus, the predictions in the composite laminates based on such parameters may disagree with experimental results for strains higher than 1%. In addition, at high strain levels, the matrix cracking/matrix failure generally occurs in off-axis plies which may also cause the stiffness degradation of the laminates.

The stress and strain curves of $[\pm 45]_{3s}$ and $[60/-30]_{3s}$ graphite/epoxy laminates obtained from the experiments were compared with the model predictions in Figs. 13 and 14, respectively. It was revealed that the strain rate effect seems to be considerable, especially in the nonlinear ranges. From the comparison, it was indicated that the viscoplasticity model provides fairly good prediction for the rate dependent nonlinearity of the laminate at strain up to 1.2%. Beyond this strain value, the experimental results tend to be

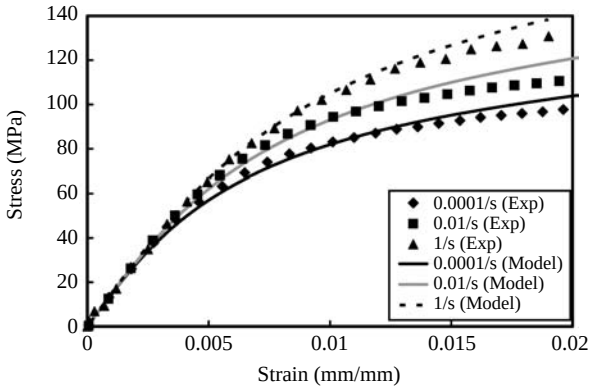

Fig. 13 Comparison of model predictions and experimental stress-strain curves for $[\pm 45]_{3s}$ graphite/epoxy laminates at three different strain rates

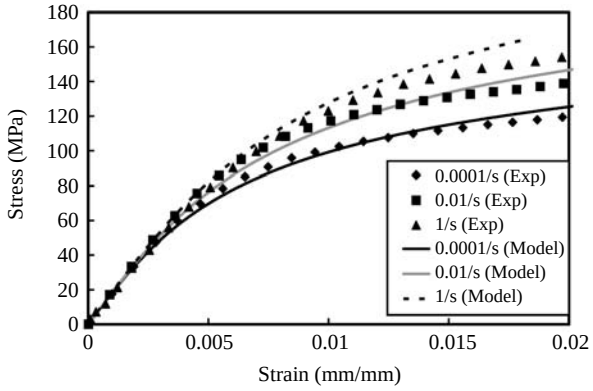

Fig. 14 Comparison of model predictions and experimental stress-strain curves for $[60/-30]_{3s}$ graphite/epoxy laminates at three different strain rates

softer than the model predictions and the degrading tendency is similar to that in the glass/epoxy composites. It is noted that in the study, the stacking sequences of the laminates were decided just by random choice without any special consideration.

VIII. CONCLUSIONS

A constitutive model was proposed based on the three parameter viscoplasticity model in conjunction with the laminated plate theory for modeling the rate dependent constitutive behaviors of composite laminates. Through a numerical iteration of the incremental form of the constitutive formulation, the stress and strain relations of the composite laminates at various strain rates were generated. Symmetric glass/epoxy composite laminates ($[\pm 45/90_2]_{4s}$ and $[75_2/-60/30]_{4s}$) and graphite/epoxy composite laminates ($[\pm 45]_{3s}$ and $[60/-30]_{3s}$) were tested in tension at three different strain rates. Experimental results show that the linear parts of the stress and strain curves are not sensitive to strain rate, however, the nonlinear portions quite definitely rely on strain rate. Comparison of the experimental data with model predictions indicates that the proposed constitutive model is capable of predicting the rate dependent behaviors of the laminates at strain levels up to 1%.

REFERENCES

Gates, T. S., and Sun, C. T., 1991. "Elastic/Viscoplastic Constitutive Model for Fiber Reinforced Thermoplastic Composites," *AIAA Journal*, Vol. 29, pp. 457-463.

Gibson, R. F., 1994, *Principles of Composite Material Mechanics*, McGraw-Hill, Inc., New York.

Hosur M. V., Alexander J., Vaidya U. K., and Jeelani S. 2001 "High Strain Rate Compression Response of Carbon/Epoxy Laminate Composites," *Composite Structures*, Vol. 52, pp. 405-417.

Lanza di Scalea, F., 1998 "Measurement of Thermal Expansion Coefficients of Composites Using Strain Gages," *Experimental Mechanics*, Vol. 38, No. 4, pp. 233-241.

Sun, C. T., and Zhu, C., 2000 "The Effect of Deformation-Induced Change of Fiber orientation on the Non-linear Behavior of Polymeric Composite Laminates," *Composites Science and Technology*, Vol. 60, pp. 2337-2345.

Sun, C. T., and Chen, J. L., 1989 "A Simple Flow Rule for Characterizing Nonlinear behavior of Fiber Composites," *Journal of Composite Materials*, Vol. 23 pp. 1009-1020.

Thiruppukuzhi, S. V., and Sun, C. T., 2001 "Model for the Strain-Rate-Dependent Behavior of Polymer Composites," *Composites Science and Technology*, Vol. 61, pp. 1-12.

Tsai, J., and Sun, C. T., 2002 "Constitutive Model for High Strain Rate Response of Polymeric Composites," *Composites Science and Technology*, Vol. 62, pp. 1289-1297.

Tuttle, M.E. 1989 "Fundamental Strain-Gage Technology", *Manual on Experiment Methods for Mechanical Testing of Composites*, edited by Pendleton, R. L and Tuttle, M.E, Society for Experimental Mechanics, Bethel, CT, USA.

Yoon, K. J., and Sun, C. T., 1991. "Characterization of Elastic-Viscoplastic Properties of an AS4/PEEK Thermoplastic Composite," *Journal of Composite Materials*, Vol. 25, pp. 1277-1298.

Manuscript Received: Oct. 13, 2005
Revision Received: Feb. 26, 2006
and Accepted: Mar. 13, 2006